NANO LETTERS

Letter

pubs.acs.org/NanoLett

Electrochemical Size Measurement and Characterization of Electrodeposited Platinum Nanoparticles at Nanometer Resolution with Scanning Electrochemical Microscopy

Wei Ma,[†] Keke Hu,[‡] QianJin Chen,[†] Min Zhou,[†] Michael V. Mirkin,[‡] and Allen J. Bard*[,†]

[†]Center for Electrochemistry, Department of Chemistry, The University of Texas at Austin, Austin, Texas 78712, United States

[‡]Department of Chemistry and Biochemistry, Queens College, City University of New York, Flushing, New York 11367, United States

Supporting Information

ABSTRACT: The properties of nanoparticles (NPs) are determined by their size and geometric structures. A reliable determination of NP dimension is critical for understanding their physical and chemical properties, but sizing ultrasmall particles on the order of nanometer (nm) scale in the solution is still challenging. Here, we report the size measurement of PtNP at nanometer resolution by *in situ* scanning electrochemical microscopy (SECM), performed with the electrochemical generation and removal of H_2 bubble at a reasonably small distance between tip and substrate electrodes in 200 or 500 mM $HClO_4$ solution. A series of different PtNPs or nanoclusters were electrodeposited and *in situ* measured in the solution, proving the concept of sizing ultrasmall particles using tip generation/substrate collection mode of SECM. This technique could be also used for investigations of other supported ultrasmall metal nanocluster systems.

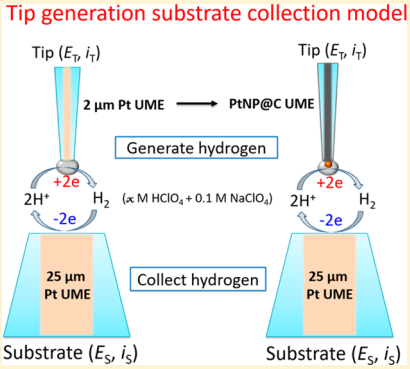

KEYWORDS: *SECM, electrochemical size measurement, nanometer resolution, platinum nanoparticles, hydrogen bubble*

Investigations of metal nanoparticles (NPs) started in 1856, when Michael Faraday prepared gold colloids by etching thin films of gold.[1] Many years later methods for synthesizing such colloids were developed, e.g. by John Turkevich.[2] Much more recently, methods for imaging such colloids became available, for example, scanning electron microscopy (SEM), and the nanoparticle nomenclature was adopted. We have been studying the electrodeposition of nanometer (nm) and sub-nm platinum (Pt) particles on inert substrates (e.g., carbon, TiO_2) and their characterization by electrochemical technique.[3] We are especially interested in forming single, isolated NPs by depositing them on ultramicroelectrode (UME) and determining the size and shape of the deposited particles by electrochemical methods. As imaging and characterization techniques, electrochemical methods have the advantage of not being diffraction limited and do not involve high-energy irradiation.[4,5] Moreover, they are capable of making measurements for electrodes, as they are prepared in solution and without the need for transfer to the gas phase or vacuum. In most cases one can make the measurements, as we describe in this letter, without extensive searching to find the particles even at the 1 nm level.

Scanning electrochemical microscopy (SECM) is a powerful technique that probes local electrochemical current by scanning with a tip electrode across the sample surface, currently with a resolution of nm scale.[6−8] SECM can be successfully used for imaging individual immobilized NPs with a nm-sized SECM probe, providing spatially resolved information about NP shape and measure its electron transfer properties and catalytic activities.[9,10] However, in this work as described below the SECM is used to prevent hydrogen bubble formation at a high proton concentration and provide a more precise limiting current for area and radius determination. In this work, we demonstrate the electrodeposition and electrochemical measurement of PtNPs from μM solution of $PtCl_6^{2-}$ with sizes of tens of nm to ∼1 nm.

The experiment as shown in Figure 1 consisted of an electrodeposition that was followed by replacement of the solution and an electrochemical analysis step to determine particle size. This deposited NP size depended on the $PtCl_6^{2-}$ concentration (10 to 100 μM) and the deposition time (a few seconds). The analysis was based on electrocatalytic amplification where proton reduction (the HER) occurs on the Pt but not on the carbon at the given potential. The electrochemical response is dependent on the concentration of perchloric acid ($HClO_4$) used. At $HClO_4$ concentrations below about 60 mM, concentration of hydrogen within the solution volume near the PtNP was not high enough to nucleate to a gaseous H_2 bubble. At higher $HClO_4$ concentrations, H_2 gas is the vault and nucleation occurs, disturbing the voltammogram. This is especially true at high proton concentrations, which are

Received: April 6, 2017
Revised: May 26, 2017
Published: June 14, 2017

DOI: 10.1021/acs.nanolett.7b01437
Nano Lett. 2017, 17, 4354−4358

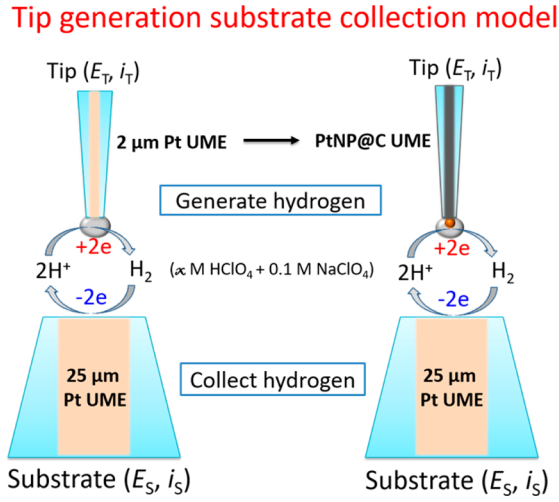

Figure 1. Schematic depiction of SECM strategy for electrochemical sizing using H_2 generation and collection by tip generation/substrate collection (TG/SC) model in different concentration of $HClO_4$ containing 0.1 M $NaClO_4$ at various distance between tip and substrate electrodes with E_S = +0.1 V vs Ag/AgCl, while E_T scans from 0 to −1.0 V vs Ag/AgCl.

useful in obtaining a high sensitivity. Formation of gas bubble will block the electrode surface and decrease the limiting current, as shown below. Thus, for larger radius PtNPs, low concentrations of protons can be used to obtain clear mass transfer controlled limiting currents from which the radius can be determined. However, for very small NPs and clusters, higher concentrations were used with steps taken to prevent bubble formation.

To illustrate the principles of these measurements, we first show results with a low concentration of acid at μm size UMEs. Typical HER steady state voltammetry of 20 mM $HClO_4$ with 0.1 M $NaClO_4$ as supporting electrolyte at a scan rate of 0.1 V·s^{-1} for a Pt disk UME (1.0 μm radius) is shown in Figure 2c and Supporting Figure S1. When the UME is far from a substrate electrode, the limiting current is given by the well-known eq 1 for a disk UME.

$$i_{lim} = 4xnFDca \quad (1)$$

where i_{lim} is a mass transfer controlled limiting current, x is a coefficient for the RG value,[16] n is the electron transfer number (= 1 for proton reduction), F is the Faraday constant (96485 C/mol), D is the diffusion coefficient of H^+ (8×10^{-5} cm^2/s), and c is the concentration of proton (20 mM).

Size from diffusion-limited currents of HER is consistent with the calculation from 0.5 mM FcMeOH solution and SEM image (Figure S2), indicating the active surface of Pt UME for proton transfer reaction. When the tip is closer to the substrate electrode under positive feedback conditions, the tip current is increased by a factor given by the approach curves (Figure 2b). Figure 2c also shows the results in the tip generation/substrate collection (TG/SC) mode where the tip and substrate electrode voltammograms are plotted at various distances, d, respectively. In the case of a 10 μm gap, the collection efficiency (CE) is around 63%, while the CE is 100% at a smaller gap of 1.0 and 0.4 μm. The generation and collection mode is also useful in aligning of tip and substrate electrodes and SECM imaging (Figure 2a).

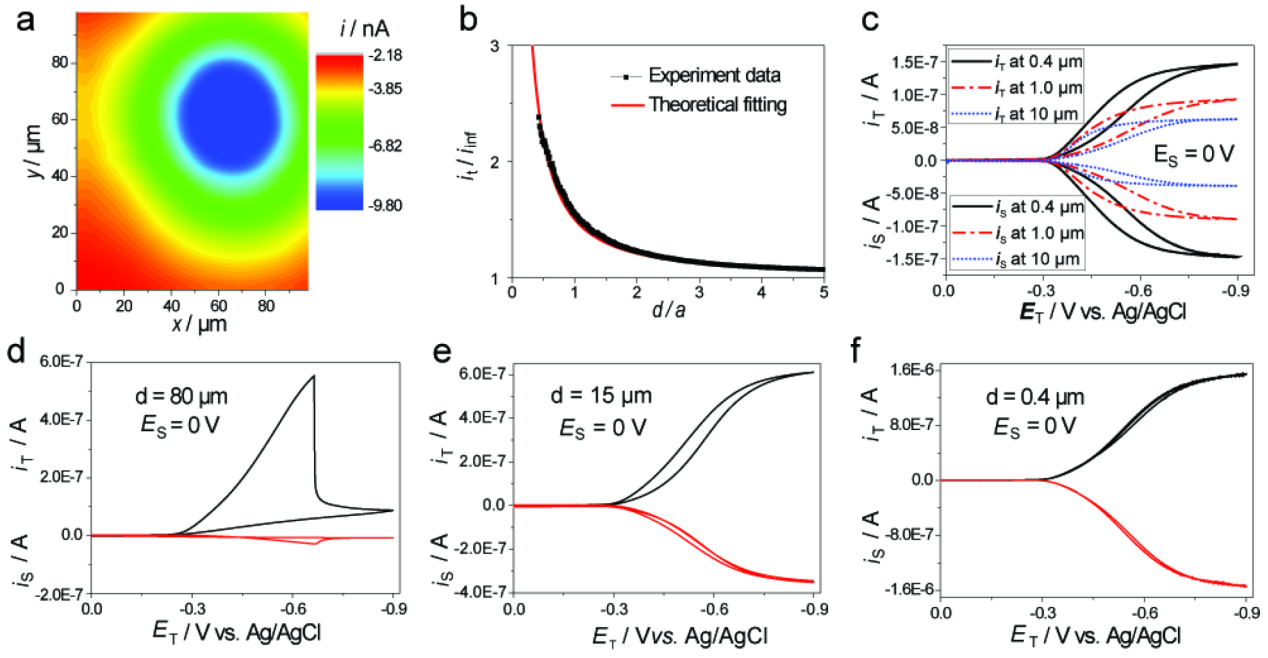

Figure 2. Electrochemical generation and collection of H_2 using the TG/SC mode of SECM. (a) SECM image with SG/TC model for alignment displaying the tip (1.0 μm radius) current for H_2 collection above a single Pt substrate electrode (12.5 μm radius) in 20 mM $HClO_4$ containing 0.1 M $NaClO_4$ with E_T = 0 V vs Ag/AgCl, while E_S = −0.9 V vs Ag/AgCl. (b) Approach curve to Pt substrate electrode (E_S = 0 V vs Ag/AgCl) obtained using 20 mM $HClO_4$ and 0.1 M $NaClO_4$ with the Pt tip with E_T = −0.9 V vs Ag/AgCl probe. (c) Generation of H_2 at Pt tip and simultaneous H_2 collection at a Pt substrate electrode at different separation distances in 20 mM $HClO_4$ with 0.1 M $NaClO_4$ solution. (d) Generation and collection of H_2 bubble at distances of 80 μm in 200 mM $HClO_4$ solution. (e,f) Generation and removal of H_2 bubble at 15 and 0.4 μm in 200 mM $HClO_4$ solution. For TG/SC mode of SECM, the E_T is scanned from 0 to −0.9 V vs Ag/AgCl at a scan rate of 100 mV·s^{-1}, while E_S is fixed at 0 V vs Ag/AgCl. Curves with black color and red color are the tip and substrate electrode voltammograms, respectively.

DOI: 10.1021/acs.nanolett.7b01437
Nano Lett. 2017, 17, 4354−4358

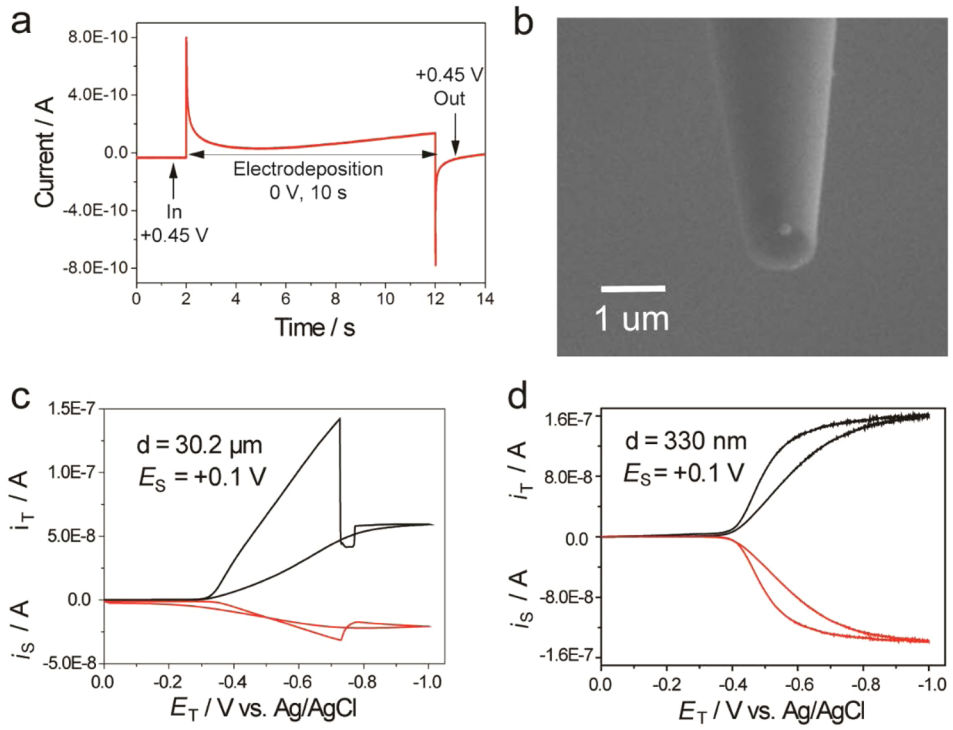

Figure 3. Electrochemical sizing of a single PtNP using SECM strategy. (a) Current−time transients of the electrodeposition of a single PtNP on C UME for 10 s in 100 μM H_2PtCl_6 and 10 mM H_2SO_4 at 0 V vs Ag/AgCl. (b) SEM image of a PtNP on C UME after deposition. (c,d) Generation and collection of H_2 bubble at distances of 30.2 μm and 330 nm in oxygen-free 200 mM $HClO_4$ solution using the TG/SC mode of SECM. The E_T is scanned from 0 to −1 V vs Ag/AgCl at a scan rate of 100 mV·s^{-1}, and E_S is held at +0.1 V vs Ag/AgCl. Curves with black color and red color are the tip and substrate electrode voltammograms, respectively.

When the $HClO_4$ concentration increased to 200 mM, rather than a sigmoidal shaped diffusion control limiting current, a peak shaped voltammogram associated with a gaseous H_2 bubble formation is observed. As shown in Figure 2d, a sharp drop of current associated with proton reduction at the tip is obtained at ∼−0.68 V vs Ag/AgCl. The H_2 concentration at the tip electrode surface from proton reduction exceeds the critical concentration for nucleation. Such a gas-phase bubble covers most of the active electrode surface, leaving a small portion of the Pt/solution interface for further proton reduction as suggested by the small steady-state residual current. Such a bubble formation behavior at a ∼1 μm radius Pt disk electrode is very similar to that at the nanodisk electrodes previously reported by White's group.[11] Note that the bubble formation behavior at the tip electrode can be also sensed at the substrate electrode with a sudden increase of current from H_2 oxidation. In our study, we focused on the sizing of small electrodes from diffusion controlled limiting current at high acid concentration based on eq 1. Our strategy is to approach the tip to the substrate electrode to a reasonably close distance so that bubble formation behavior can be prevented due to a H_2 pump effect at the substrate electrode by oxidation. As shown in Figure 2e, a steady state diffusion controlled limiting current is attained at a distance of 15 μm, from which the radius of the tip electrode can be recalibrated to be 0.93 μm based on eq 1, consistent with results from bulk electrochemistry. As the distance becomes smaller (Figure 2f), a similar sigmoidal shaped voltammetry is obtained. However, there is a significant (∼2.7) feedback in terms of the tip current at a distance of $L = d/a = 0.4$. In the remaining content, we rely on the diffusion limited current at the region where there is no significant feedback to calibrate the size of electrode.

After demonstrating bubble collection by the substrate electrode at a reasonably close distance, we now consider the electrochemical sizing of NPs, which are electrodeposited at a carbon UME (C UME). The SECM cell was modified with two inlet and outlet tubes for solution injection and removal. This allows the distance calibration from the approach curves based on FcMeOH, followed by the solution swap from electrodeposition to electrocatalytic analysis solution. We showed by SECM measurements that solution replacement could be carried out, as described below, without appreciable change in the position of the tip electrode with respect to the substrate electrode. However, considering the inevitable drift of positioners over experimental time, the absolute value of the distances, especially at very small range, are recalibrated based on the theoretical calculated CE using COMSOL simulation (details for the CE simulation in a different PtNPs case can be found in the Supporting Information).

The electrodeposition of a single PtNP was carried out at the C UME by holding it at a rest potential of +450 mV vs Ag/AgCl and then applying a potential pulse to 0 V vs Ag/AgCl for several seconds from a solution of 100 μM H_2PtCl_6 in 10 mM H_2SO_4 (Figure 3a).[12,13] Typically, the deposition transient current showed a fast charging pulse followed a period over which the current maintains a very low value and then the current increases gradually, corresponding to $PtCl_6^{2-}$ diffusion to the growing PtNP.[14] Assuming a spherical geometry and a current efficiency for deposition of 100%, we can estimate the radius of the deposited PtNP, r_{NP}, from the integrated current by eq 2.

DOI: 10.1021/acs.nanolett.7b01437
Nano Lett. 2017, 17, 4354−4358

$$r_{NP} = \sqrt[3]{\frac{3QV_a}{4\pi nq}} \quad (2)$$

where Q is the integrated charge from experimental current transient charge (corrected for the double layer charge), V_a is the atomic volume of Pt (2.32×10^{-29} m^3), n is the number of electrons transferred per Pt atom (n = 4), and q is the elementary charge. In most cases only a single PtNP was formed on the electrode surface as observed by SEM as typical for depositions on UMEs.[13] For example, a single PtNP with a radius of 108 nm was observed with nearly spherical geometry by SEM (Figure 3b). This is close to the value (134 nm) estimated from the integrated charge (see Table 1), justifying the assumption of spherical shape for the PtNP.

Table 1. Parameters for Deposition of a Single PtNP or Cluster at an FIB-Milled C UME and Comparison of the Radii Estimated from the Integrated Charge, Limiting Current and SEM Result

C UME radius (nm)	$[H_2PtCl_6]$ (μM)	deposition time (s)[a]	r_{NP} from Q (nm)[b]	$[HClO_4]$ (mM)	r_{NP} from i_{lim} (nm)[c]	r_{NP} from SEM (nm)[d]
335	100	5	65	20	63	64
360	100	10	134	200	117	108
290	100	5	61	200	59	58
300	100	3	33	200	39	41
130	30	10	[e]	500	7.8	
175	30	10		500	7.1	
150	30	10		500	5.7	
195	10	10		500	3.5	
215	10	5		500	1.8	

[a]Duration time at the applied potential of 0 V Ag/AgCl for deposition. [b]Size of deposited PtNP from the integrated charges assuming a spherical geometry and 100% deposition efficiency. [c]Radius of deposited PtNP on the C UME surface was estimated from the steady-state current obtained voltammograms in $HClO_4$ solution assuming a single PtNP with a spherical geometry on a planar surface. [d]Size of deposited PtNP from SEM results. [e]Not applicable because deposition current at pA level was overwhelmed by the system noise.

After PtNP electrodeposition, the solution in the SECM cell was then replaced by one for analysis observing the HER in 200 mM $HClO_4$. Although electrodeposited particles can also be studied with 20 mM H^+ without perturbation of gaseous bubble formation, a higher sensitivity can be obtained with larger acid concentrations (200 mM or 500 mM H^+). In our previous study of particle collision, the spike current feature associated with H^+ reduction was observed when single PtNP collided at the C UME.[15] Such a current spike may be attributed to H_2 bubble formation at the PtNP even in lower proton concentration. Figure 3c shows when the tip is far away from the substrate electrode (d = 30.2 μm), a gaseous bubble formation behavior (although not as well behaved as disk electrodes in Figure 1) is observed. Interestingly, when the tip was approached close the substrate electrode (d = 330 nm), the substrate electrode functioned as a H_2 pump, preventing the formation of gaseous H_2 bubble at the tip. The resulting diffusion limited current enables the estimation of the PtNP size at the C UME tip based on the following eq 3, assuming the deposit is a sphere.

$$i_{lim} = 4\pi \ln(2) nFDCr_{NP} \quad (3)$$

where i_{lim} is a steady-state current, n is the electron transfer number (=1 for proton reduction), F is the Faraday constant (96485 C/mol), D is the diffusion coefficient of H^+ (8×10^{-5} cm^2/s), and c is the concentration of proton. If the deposit is hemispherical, the geometric term 4π (ln 2) is replaced by 2π. The measured steady-state current about 158 nA at a PtNP deposited C UME in Figure 3d leads to a spherical PtNP with radius of 117 nm. Notably, the estimated size is in good agreement with both the integrated charge (134 nm) and the SEM measurement (108 nm). We further demonstrate the validity of voltammetric characterization for PtNP size by a steady-state current of HER (Figure S3).

An even higher sensitivity is obtained in 500 mM acid (Figure 4 and Figure S4–6). The smaller NPs were generated

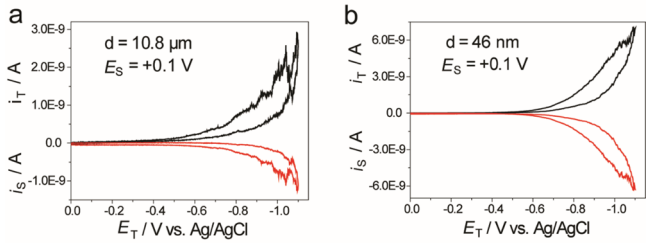

Figure 4. Generation and collection of H_2 bubble at a single Pt cluster, r_{NP} = 1.8 nm using SECM at distances of 10.8 μm (a) and 46 nm (b) in an oxygen-free 500 mM $HClO_4$ solution. The E_T is scanned from 0 to −1.1 V vs Ag/AgCl at a scan rate of 100 mV·s^{-1}, and E_S is held at +0.1 V vs Ag/AgCl. Curves with black color and red color are the tip and substrate electrode voltammograms, respectively. The radius of the nanoparticle was obtained from the diffusion current shown in (b) by use of eq 3.

with a lower concentration of $PtCl_6^{2-}$ and shorter plating pulses. The use of the nano-SECM[6] was necessary and provided better stability and smaller tip drift. Table 1 summarizes the electrodeposition and electrochemical analysis conditions as well as estimates of particle size from the plating current and the diffusion limiting current. For the smaller NP deposits, the plating current was too small to allow reasonable estimates. In general, however, we find good agreement between the two estimates and also that from several SEM images.

Results with the smallest particle examined, radius 1.8 nm, are shown in Figure 4. Note that when the tip was far from the substrate electrode, the characteristic peak associated with H_2 bubble formation occurred (Figure 4a). When the tip was moved closer to the substrate electrode, d = 46 nm, such bubble formation was not seen, and a relatively smooth diffusion-limited current was obtained (Figure 4b). Note that although the distance between tip and substrate electrodes is very small, the relative distance ($L = d/a$ = 25.5) is still too large for measurable current feedback. These results are consistent with the model of nanobubble formation, even at very small NPs. Note that such an SECM tip with a single small PtNP on C UME has extremely large RG-value (where RG is the ratio of the carbon tip to the Pt particle radius). We do not yet fully understand the mechanism of how the H_2 pump at the substrate electrode can prevent the bubble formation at the tip and further investigation on this is under way in our group.

Previously, White and co-workers have studied the formation of hydrogen nanobubbles on Pt disk electrodes inlaid in glass capillaries, including bubble nucleation, growth, dynamics, and

DOI: 10.1021/acs.nanolett.7b01437
Nano Lett. 2017, 17, 4354–4358

stability.[17−21] Experiment for proton reduction in 0.5 M H_2SO_4 with disks of 1 to 50 nm radii (measured from limiting current of Fc/Fc^+) shows the characteristic sharp peak with the rapid current decay to small background levels. A plot of the height of the current peak with disk radius produced a linear correlation (black square, Figure 5). Also shown in this figure are plots of

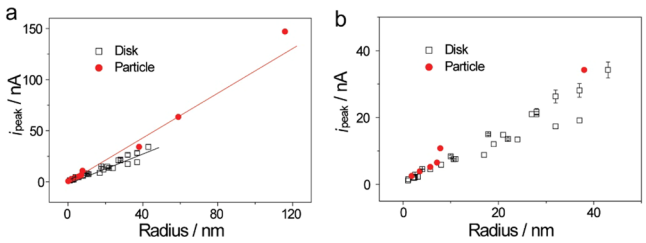

Figure 5. H_2 bubble peak current, i_{peak}, as a function of particle (red circle) and disk (black square) radii (a) from 1 to 117 nm and (b) from 1 to 45 nm (a magnified area in panel a). Data of Pt nanodisk electrode adapted from ref 18.

peak found in this study of electrodeposited particles (red circle, Figure 5). Even though there are considerable differences in the Pt structure and geometry, as well as the C substrate, the results are very close to each other over the radii shown. We can also compare the relative supersaturation needed for nanobubble formation, $C_{H_2,crit}/C_{eq}$, where $C_{H_2,crit}$ is the critical surface concentration of dissolved H_2 required for nanobubble nucleation and C_{eq} is the equilibrium concentration (0.8 mM at room temperature). $C_{H_2,crit}$ can be estimated from the peak current, assuming controlled diffusion from the equation $i_{peak} = 4\pi(\ln 2)nFD_{H_2}C_{H_2,crit}r_{NP}$, where D_{H_2} is the diffusion coefficient of H_2 (4.5×10^{-5} cm^2/s), r_{NP} is the particle radius, and n (= 2) is the number of electrons transferred per a H_2 molecule. This yields $C_{H_2,crit} \approx 0.17$ M and a H_2 supersaturation at the PtNP surface for nanobubble nucleation of ~210, which is in reasonable agreement with that at a nanodisk of ~310.

We have shown that it is possible to prepare PtNP down to 1 nm dimensions by electrode deposition on a carbon substrate. It is also possible, without removing the electrode from an aqueous environment, to obtain the size of the particle by observing the electrochemical reduction of protons to hydrogen. Conditions are described by employing a scanning electrochemical microscope to prevent the formation of gas bubbles on the electrode surface. The results also confirm that blocking effects on PtNPs are indeed the result of hydrogen bubble formation. Analogous experiments should be possible with other systems to produce a variety of metal and metal oxide NPs.

■ ASSOCIATED CONTENT

Supporting Information

The Supporting Information is available free of charge on the ACS Publications website at DOI: 10.1021/acs.nanolett.7b01437.

Experiment details; fabrication and characterization of FIB-milled UME; deposition of a PtNP; SECM measurement; geometry, meshes, boundary conditions, and report of finite-element simulation (PDF)

■ AUTHOR INFORMATION

Corresponding Author

*E-mail: ajbard@cm.utexas.edu.

ORCID

Allen J. Bard: 0000-0002-8517-0230

Author Contributions

All authors have given approval to the final version of the manuscript. W.M. performed all electrochemical experiments, analyzed the data, and wrote the manuscript. K.K.H. prepared C UME. Q.J.C., M.Z., and M.V.M. did simulation work and discussed the data. A.J.B. conducted the research, analyzed the data, and cowrote the manuscript.

Notes

The authors declare no competing financial interest.

■ ACKNOWLEDGMENTS

We acknowledge support of this research from the AFOSR MURI (FA9550-14-1-0003), National Science Foundation (CHE-1405248, to A.J.B.; CHE-1300158, to M.V.M.), and the Robert A. Welch Foundation (F-0021).

■ REFERENCES

(1) Faraday, M. *Philos. Trans. R. Soc. London* **1857**, *147*, 145−181.
(2) Turkevich, J.; Stevenson, P. C.; Hillier, J. *J. Phys. Chem.* **1953**, *57*, 670−673.
(3) Kim, J.; Dick, J. E.; Bard, A. J. *Acc. Chem. Res.* **2016**, *49*, 2587−2595.
(4) Li, Z. Y.; Young, N. P.; Di Vece, M.; Palomba, S.; Palmer, R. E.; Bleloch, A. L.; Curley, B. C.; Johnston, R. L.; Jiang, J.; Yuan, J. *Nature* **2008**, *451*, 46−48.
(5) Gontard, L. C.; Fernández, A.; Dunin-Borkowski, R. E.; Kasama, T.; Lozano-Pérez, S.; Lucas, S. *Micron* **2014**, *67*, 1−9.
(6) Kim, J.; Renault, C.; Nioradze, N.; Arroyo-Currás, N.; Leonard, K. C.; Bard, A. J. *Anal. Chem.* **2016**, *88*, 10284−10289.
(7) Takahashi, Y.; Kumatani, A.; Shiku, H.; Matsue, T. *Anal. Chem.* **2016**, *89*, 342−357.
(8) Kim, J.; Renault, C.; Nioradze, N.; Arroyo-Currás, N.; Leonard, K. C.; Bard, A. J. *J. Am. Chem. Soc.* **2016**, *138*, 8560−8568.
(9) Sun, T.; Yu, Y.; Zacher, B. J.; Mirkin, M. V. *Angew. Chem., Int. Ed.* **2014**, *53*, 14120−14123.
(10) Blanchard, P.-Y.; Sun, T.; Yu, Y.; Wei, Z.; Matsui, H.; Mirkin, M. V. *Langmuir* **2016**, *32*, 2500−2508.
(11) Luo, L.; White, H. S. *Langmuir* **2013**, *29*, 11169−11175.
(12) Chen, S.; Kucernak, A. *J. Phys. Chem. B* **2003**, *107*, 8392−8402.
(13) Kim, J.; Bard, A. J. *J. Am. Chem. Soc.* **2016**, *138*, 975−979.
(14) Velmurugan, J.; Noel, J.-M.; Mirkin, M. V. *Chem. Sci.* **2014**, *5*, 189−194.
(15) Xiao, X.; Bard, A. J. *J. Am. Chem. Soc.* **2007**, *129*, 9610−9612.
(16) Kim, J.; Bard, A. J. *Anal. Chem.* **2016**, *88*, 1742−1747.
(17) Chen, Q.; Luo, L.; White, H. S. *Langmuir* **2015**, *31*, 4573−4581.
(18) Chen, Q.; Luo, L.; Faraji, H.; Feldberg, S. W.; White, H. S. *J. Phys. Chem. Lett.* **2014**, *5*, 3539−3544.
(19) German, S. R.; Chen, Q. J.; Edwards, M. A.; White, H. S. *J. Electrochem. Soc.* **2016**, *163*, H3160−H3166.
(20) Luo, L.; White, H. S. *Langmuir* **2013**, *29*, 11169−1175.
(21) German, S. R.; Edwards, M. A.; Chen, Q.; White, H. S. *Nano Lett.* **2016**, *16*, 6691−6694.

DOI: 10.1021/acs.nanolett.7b01437
Nano Lett. 2017, 17, 4354−4358